Fluorescence Analysis of Single and Mixed Micelle Systems of SDS and DTAB

Kerry K. Karukstis,* Steven W. Suljak, Petra J. Waller, Jennifer A. Whiles, and Elizabeth H. Z. Thompson

Department of Chemistry, Harvey Mudd College, Claremont, California 91711

Received: April 2, 1996; In Final Form: April 25, 1996[⊗]

Structural features of the single and mixed micellar systems of sodium dodecyl sulfate (SDS) and dodecyltrimethylammonium bromide (DTAB) were characterized using the fluorescence probe 6-propionyl-2-(dimethylamino)naphthalene (Prodan). In particular, our investigations capitalized on the spectral sensitivity of Prodan to its environment as well as the extensive solubility of Prodan in solvents of varying polarity and/or hydrophobicity to effectively use a three-mode factor analysis technique to resolve the coincident emission from Prodan in multiple microenvironments of single and mixed micelle systems. Our investigations reveal parameters of Prodan fluorescence that reflect the relative polarities of the surfaces of SDS and DTAB micellar cores, the permeability of the SDS micelle interface, and the heterogeneity of SDS−DTAB mixed micellar systems. In particular, we observe a strong affinity of Prodan for both SDS and DTAB micelles at the water−surfactant interface with the emission λ_{max} of Prodan consistent with greater water accessibility in the SDS interfacial region. Reduction in SDS head-group repulsion upon the addition of both an alkali metal series of counterions ($Li^+ \rightarrow Na^+ \rightarrow K^+$) and a tetrasubstituted ammonium series of counterions ($NH_4^+ \rightarrow N(CH_3)_4^+ \rightarrow N(CH_3CH_2)_4^+ \rightarrow N(CH_3CH_2CH_2CH_2)_4^+$) appears to induce a more nonpolar environment for Prodan. Each one-phase and two-phase region of the dilute aqueous binary SDS−DTAB pseudoternary diagram is identified by distinct Prodan λ_{max} values. Evidence is presented for the presence of SDS−DTAB mixed micelle systems.

Introduction

Incorporation of molecular probes into aqueous micelles effectively reveals such parameters as the critical micelle concentration (cmc), roughness of the micelle surface, and degree of water penetration into these surfactant aggregations. Many studies employ molecular probes with fluorescence characteristics that reflect their microenvironment. Attributes such as fluorescence intensity values, excitation and emission wavelength maxima, and fluorescence lifetime and polarization values are potential indicators of the features of a probe's surroundings. Most probes have been chosen for their particular affinity for one or two of the principal micelle regions: the hydrocarbon core formed from surfactant tails, the interface composed primarily of the amphiphile head groups, or the surrounding aqueous solvent phase. Selective targeting of specific micellar domains has been precisely achieved with fluorophores such as polycyclic aromatic hydrocarbons (e.g., pyrene, naphthalene, and anthracene) and with ionic derivatives of aromatic chromophores (e.g., pyrenesulfonic acid, pyrenebutyric acid, and 1-anilinonaphthalene-8-sulfonate).[1]

However, the probe 6-propionyl-2-(dimethylamino)naphthalene (Prodan) is a novel molecular reporter with potential added advantages for a new approach to micelle characterization. Prodan is soluble in an extensive range of media, suggesting the possibility of the simultaneous partitioning of the probe into all regions of the micelle. This neutral, hydrophobic probe displays appreciable shifts in the wavelength of maximum emission with a variation in solvent, enabling the location of the probe in distinct regions to be established. For example, maximal fluorescence emission ranges from 400 nm in the nonpolar solvent cyclohexane to 530 nm in aqueous solution. In addition to this spectral sensitivity, Prodan has the advantage of exhibiting measurable fluorescence intensities in both polar and apolar solvents. Thus, fluorescence signatures from a location in the bulk solvent as well as within the various microenvironments of a surfactant aggregation are ascertainable. Both the polarity-dependent spectral shift and the fluorescence intensity variation enable the fluorescence contributions from multiple populations of probe molecules to be easily resolved.[2,3] A further advantage of Prodan over other common probes such as 1-anilinonaphthalene-8-sulfonate (1,8-ANS) is the absence of a permanent charge, eliminating complications from ionic interactions.[2]

The surfactants sodium dodecyl sulfate (SDS) and dodecyltrimethylammonium bromide (DTAB) constitute an interesting system to study as both single and mixed micelle systems. The anionic SDS and the cationic DTAB possess identical hydrocarbon tails (12-carbon alkyl chains) but oppositely charged head groups. These single-chain surfactants with relatively large head-group areas form spherical micelles of low polydispersity in aqueous solution.[4] For SDS, a cmc value at 25 °C of 8.1 mM is generally well accepted[5−8] but a wide range of values from 56 to 80 have been reported for the measured aggregation number N under comparable experimental conditions.[5,7,9,10] Similarly, a rather constant cmc value of 14.8−15.6 mM[5,8,11] but a variable aggregation number ranging from 43 to 74[5,9,11] are characteristic of DTAB micelles at 25 °C. For both SDS and DTAB, aggregation number and the polydispersity of the sample increase as the concentration of surfactant increases above the cmc.[4] Measurements under the same conditions consistently reveal a larger aggregation number for SDS micelles than for DTAB aggregates (e.g., 80 for SDS vs 50 for DTAB,[5] 64 for SDS vs 55 for DTAB,[12] and 77 for SDS vs 74 for DTAB[9]). With increased ionic strength (e.g., high $[Na^+]$ for SDS, high $[Br^-]$ for DTAB), the micelles undergo substantial transformations in size and shape to create cylindrical micelles with large aggregation numbers. For example, aggregation numbers for SDS micelles at 25 °C in the presence of increasing [NaCl]

[⊗] Abstract published in *Advance ACS Abstracts,* June 1, 1996.

S0022-3654(96)00993-8 CCC: $12.00

steadily increase: for [NaCl] = 0.1, 0.2, and 0.4 M, N = 91, 105, and 129, respectively.[7] DTAB micelles show a corresponding (but less dramatic) increase in aggregation number with added NaBr: N = 71, 76, and 78 at [NaBr] = 0.0175, 0.05, and 0.10 M, respectively.[11]

The phase behavior of dilute (<5 wt % surfactant) aqueous mixtures of SDS and DTAB at 25 °C has previously been characterized via a pseudoternary diagram.[9] This phase diagram is dominated by two micellar one-phase regions and two two-phase regions consisting of a 1:1 crystalline precipitate and an isotropic solution of micelles or vesicles. The single-phase micellar regions contain DTAB- and SDS-rich micelles. The region of the phase diagram constituting the DTAB-rich mixtures begins with the two-component solution of DTAB at its cmc in water (0.46 wt %) and extends to the three-component solution with an SDS/DTAB weight ratio of approximately 0.15. In this isotropic region the aggregation number of the micelles shows limited growth from 74 for pure DTAB to 111 for the system of SDS/DTAB weight ratio of 0.10. Almost all of the added anionic dodecyl sulfate ion becomes incorporated within the mixed micelle. A two-phase region of isotropic micellar liquid and crystalline equimolar precipitate exists for SDS/DTAB weight ratios between 0.15 and 1.0. The SDS-rich micelle region is demarcated by the two-component aqueous solution of SDS at its cmc (0.23 wt %) to the three-component solution with an SDS/DTAB weight ratio of approximately 1.86. As DTAB is added to SDS in this isotropic region, micelles show substantial growth in aggregation number from 77 for pure SDS to 210 for a 4:1 SDS−DTAB mixture. This increase in micelle size is attributed to the incorporation of all of the added cationic dodecyltrimethylammonium ions within the predominantly SDS micelle to reduce head-group repulsion. A narrow two-phase region of isotropic micellar solution and solid equimolar precipitate exists for SDS/DTAB ratios between 1.0 and 1.5. SDS/DTAB mixing ratios between 1.5 and 1.86 lead to a one-phase vesicle region at high water concentrations and a multiphase region also containing vesicles as the water content is lowered.

To isolate the coincident emission from Prodan in multiple microenvironments of single and mixed micelle systems, we employ fluorescence data analysis techniques capable of resolving the emission from a mixture of fluorophores. Our method of data analysis, known as the PARAFAC trilinear model,[13] is a three-mode factor analysis that enables the resolution of distinct yet overlapping excitation and emission spectra for each fluorescing component in a mixture of fluorophores. This mathematical tool permits a determination of the number of fluorescent components and their individual excitation and emission spectra without prior knowledge of either the individual components or their spectra. The basis for this technique is that the overall fluorescence intensity of a mixture of fluorophores is separately linear in functions of excitation wavelength, emission wavelength, and any parameter that alters fluorescence quantum yield or fluorophore concentration. In mathematical terms, trilinear analysis decomposes a three-way array into a sum of products of parameters using nonlinear least-squares techniques. The computational methods yield excitation and emission spectra for each fluorescing component as well as a concentration curve to establish the relative amounts of the fluorescing components. In this application, then, this mathematical tool permits a determination of the number of distinct Prodan environments and the individual excitation and emission spectra that characterize each population of Prodan molecules.

Our investigations demonstrate that Prodan is a sensitive indicator of both static and dynamic features in SDS and DTAB single and mixed micelle systems. In particular, the emission λ_{max} of Prodan fluorescence and the variable distribution of the probe reveal the microviscosity of the micelle−water interface, the permeability of the lipid−water boundary, the degree of water penetration into the micelle shell, and the extent of separation of micellar head groups.

Experimental Section

Reagents Used. Fluorescent probe 6-propionyl-2-(dimethylamino)naphthalene (Prodan, Molecular Probes, Eugene, OR) and surfactants sodium dodecyl sulfate and dodecyltrimethylammonium bromide (Aldrich) were used without further purification. Investigations that focused on the permeability of SDS micelles employed the following reagents (supplied from Aldrich unless otherwise noted): sodium salts of chloride, sulfate, and acetate ions (EM Science); benzyl alcohol (Mallinckrodt, analytical grade); chloride salts of ammonium, tetramethylammonium, tetraethylammonium, and tetrabutylammonium ions. Quenching studies employed sodium iodide and tetrabutylammonium iodide (Eastman) as quenchers. To examine the solvent dependence of Prodan emission, solvents of the highest available purity were obtained commercially from Aldrich and J. T. Baker and were used without further purification. All aqueous solutions were prepared using 18.2 MΩ ultrapure water obtained from a Milli-Q Plus Millipore water filtration system.

Protocols To Examine Features of Single-Surfactant Micelles. (a) cmc Values. We conducted investigations with varying surfactant concentration in order to confirm the cmc value for each surfactant and estimate the polarity of the micellar interface. Surfactant concentrations ranged from 0 to 18 mM for SDS and from 0 to 3 mM for DTAB. All micellar solutions were allowed to equilibrate overnight. Prodan (5 μM) was added prior to fluorescence measurements, with micellar equilibrium and probe partitioning presumed to be established by the absence of any time-dependent variation in Prodan fluorescence.

(b) Probe Distribution within SDS Micellar Regions. We also examined the effect of varying the order of addition of reagents so that Prodan was (a) added to samples after micelle formation (i.e., standard order of addition) and (b) present in solution prior to micelle formation by adding the surfactant to aqueous solutions of probe. SDS was added to water (experiment a) or aqueous solutions of Prodan (experiment b) to yield final concentrations of [SDS] = 18 mM. Trilinear analyses were performed for variable [Prodan] values from 2 to 14 μM.

(c) Reductions in the Accessibility of the Micellar Interface to Water. We also examined methods to reduce the degree of water penetration within the micelle and/or trap Prodan in the interior of the micelle by adding counterions (Li^+, Na^+, K^+, NH_4^+, $N(CH_3)_4^+$, $N(CH_3CH_2)_4^+$, and $N(CH_3CH_2CH_2CH_2)_4^+$) to reduce the electrostatic repulsion between the SDS surfactant head groups. All cations were added as the chloride salt up to 0.40 M for Li^+, Na^+, NH_4^+, $N(CH_3)_4^+$, and $N(CH_3CH_2)_4^+$, to 0.075 M for $N(CH_3CH_2CH_2CH_2)_4^+$, and to 0.010 M for K^+. Investigations involved micellar samples with [SDS] fixed at 10 mM. Counterion was added prior to the addition of Prodan probe.

We also examined the effect of the identity of the anion coupled with the added sodium counterion. Investigations involved micellar samples with [SDS] fixed at 18 mM and added sodium chloride, sodium acetate, or sodium sulfate. As sulfate anions (added as the sodium salt) and benzyl alcohol are known to increase micelle permeability by adsorbing at micellar interfaces and driving surfactant head groups further apart,[1] we

also measured the Prodan fluorescence parameters of SDS micelles treated with benzyl alcohol. Benzyl alcohol concentrations ranged from 0.05 to 0.30 M, and the concentrations of NaCl, $NaOOCCH_3$, and Na_2SO_4 ranged from 0.05 to 0.40 M.

(d) Use of Iodide as a Collisional Quencher. To enhance the identification of Prodan molecules situated in a more nonpolar position within the micelle, we used iodide ion as a collisional quencher to reduce the emission from Prodan in the more accessible regions of the micelle. The remaining fluorescence spectrum should reveal a greater contribution of the inaccessible probe molecules. NaI (up to 0.40 M) was added to SDS micelles at [SDS] = 10 mM. To distinguish the contribution to the overall fluorescence signal of the effect of added Na^+ counterion, fluorescence emission spectra were also recorded for SDS micelles treated with similar concentrations of NaCl.

Systems of SDS−DTAB Mixed Micelles. SDS−DTAB mixed micellar solutions were prepared by a simultaneous addition of both surfactants and fluorescence probe in the requisite amounts to Millipore water. Four regions of the SDS−DTAB−water dilute solution ternary diagram were explored: the one-phase region of DTAB-rich micelles (weight ratio of SDS/DTAB between 0.040 and 0.13), the one-phase region of SDS-rich micelles (weight ratio of SDS/DTAB between 3.0 and 8.0), the two-phase region of DTAB-rich micelles and DTAB−SDS precipitate (weight ratio of SDS/DTAB between 0.25 and 0.70), and the two-phase region of SDS-rich vesicles and DTAB−SDS precipitate (weight ratio of SDS/DTAB between 1.10 and 1.35). After standing overnight, solutions containing the equimolar SDS−DTAB precipitate were centrifuged to separate the solid material prior to fluorescence measurements of the remaining solution. Samples contained 10 μM Prodan for fluorescence measurements.

Fluorescence Measurements. Fluorescence spectra were obtained at 25 °C using Perkin-Elmer LS-5 and LS-50B fluorescence spectrophotometers. Excitation wavelengths were varied in 10-nm increments from 280 to 360 nm, and emission spectra were recorded over the range from 400 to 550 nm. Excitation and emission slit widths were set at 5 nm. For investigations of SDS micelles treated with benzyl alcohol, shifts in the Prodan emission spectrum prompted an adjustment in the scan parameters to the following ranges: excitation wavelengths from 330 to 410 nm and emission wavelengths from 440 to 550 nm.

Data Analyses via Trilinear Analysis. From the recorded emission spectra at the nine fixed excitation wavelengths, fluorescence intensities were determined at 5-nm intervals over the emission wavelength range. For trilinear analyses, the data were organized into a matrix of nine excitation wavelengths, 31 emission wavelengths, and seven to nine surfactant, counterion, or quencher concentrations. Nonlinear least-squares fits to the trilinear model were performed on a VAX8600. Each data set was tested for the best fit to a system of one to four fluorescing components.

Results

Resolution of Prodan Fluorescence in Several Solvents. To establish the solvent dependence of Prodan emission, we examined the emission of Prodan in several solvents of varying polarity: water, deuterium oxide, ethanol, decanol, dimethyl sulfoxide, dimethylformamide, *p*-dioxane, cyclohexane, and heptane. Table 1 summarizes the characteristics of the major emission bands resolved in each solvent. In particular, we observed the sensitivity of the emission maxima of Prodan to solvent conditions as previously demonstrated by Weber and Farris.[2]

TABLE 1: Characteristics of Prodan Fluorescence in Various Solvents

	λ_{exc}/nm[a]	λ_{em}/nm[b]
water	351	522
	287	433
deuterium oxide	360	522
	292	436
ethanol	360	488
decanol	360	470
dimethyl sulfoxide	360	466
dimethylformamide	353	461
p-dioxane	347	426
cyclohexane	340	402
	280	395
heptane	342	402
	280	393

[a] Uncertainty in excitation wavelength maximum ±1 nm. Determination of excitation wavelength maximum restricted to the wavelength range experimentally employed, 280−360 nm. [b] Uncertainty in emission wavelength maximum ±1 nm.

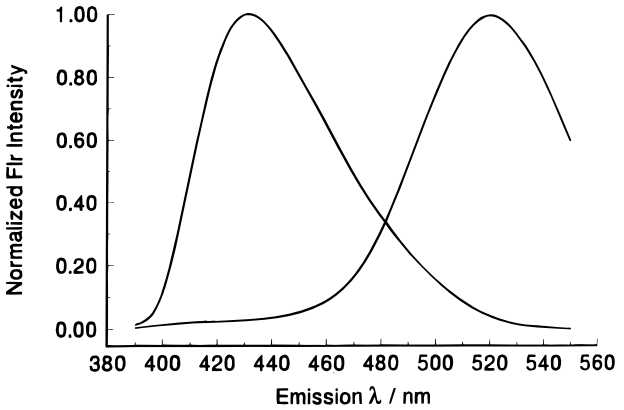

Figure 1. Resolution of the Prodan fluorescence spectrum in water into two contributing components. The normalized emission spectra are presented for the predominant component (C1) with an excitation maximum of 351 ± 1 nm and an emission maximum of 522 ± 1 nm and the minor component (C2) with an excitation maximum at 287 ± 1 nm and an emission maximally at 433 ± 1 nm.

Trilinear analysis of fluorescence data acquired in water revealed two distinct fluorescence components illustrated in Figure 1. The predominant component (C1) at longer wavelength has an excitation maximum of 351 ± 1 nm and an emission maximum of 522 ± 1 nm. The fluorescence of the shorter wavelength component (C2) is excited at 287 ± 1 nm and is emitted maximally at 433 ± 1 nm. The minor short-wavelength component has been attributed to solute−solvent complexes formed via hydrogen bonding.[14] These two fluorescence components were also observed in D_2O: C1 at λ_{exc} = 360 ± 1 nm and λ_{em} = 522 ± 1 nm and C2 at λ_{exc} = 292 ± 1 nm and λ_{em} = 436 ± 1 nm. The relative contribution of C2 is significantly reduced in D_2O.

Two distinct components were also resolved by trilinear analysis for Prodan in both heptane and cyclohexane. The components in heptane were characterized by excitation maxima of 280 and 342 nm and emission maxima of 393 and 402 nm, respectively. In cyclohexane, the parameters of the fluorescence components were quite similar, with excitation maxima of 280 and 340 nm and emission maxima of 395 and 402 nm, respectively. These two emission bands have been attributed to the presence of two closely spaced $\pi \rightarrow \pi^*$ transitions in the absorption spectrum of Prodan in various solvents.[15] All wavelengths have uncertainties of ± 1 nm.

The fluorescence data acquired for solutions of Prodan in all other solvents revealed a single component (C1) of varying

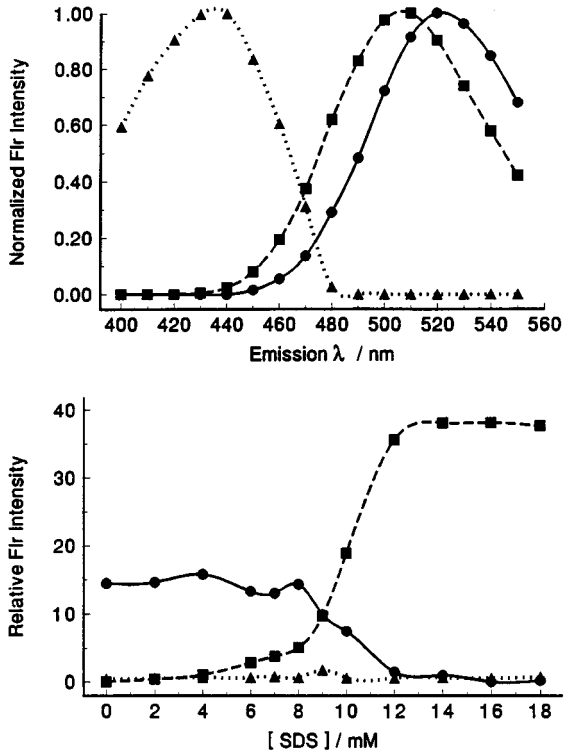

Figure 2. Resolution of the fluorescence of Prodan in aqueous SDS solutions at 25 °C into three components corresponding to emission from hydrogen-bonded Prodan molecules (▲), non-hydrogen-bonded Prodan molecules (●), and Prodan molecules interacting with micelles (■). The three resolved components are characterized by normalized emission spectra and fluorescence intensities as a function of [SDS].

emission wavelength decreasing in the order ethanol > decanol > dimethyl sulfoxide > dimethylformamide > dioxane.

Prodan Emission as a Function of [SDS]. Fluorescence studies varying the SDS concentration revealed a significant increase in Prodan fluorescence above 8 mM SDS. Trilinear analyses of the emission spectra yielded a three-component fit with Prodan emission at 433 ± 1 (λ_{exc} = 287 ± 1 nm), 507 ± 1 ($\lambda_{exc} \geq$ 360 nm), and 521 ± 1 nm (λ_{exc} = 355 ± 2 nm). Figure 2 presents the normalized emission spectra of the three components resolved by trilinear analysis as well as the intensity of each fluorescence component as a function of [SDS]. The emission peak at 521 nm dominates at [SDS] below the cmc, contributing 90 ± 4% to the overall fluorescence observed at 2 mM SDS. The intensity of the 507-nm component rises dramatically above the cmc with 96.9 ± 0.8% of the overall fluorescence arising from this component. The 433-nm emission is negligible at all [SDS], contributing 2.8 ± 0.3% to the overall fluorescence intensity at 2 mM SDS and decreasing to an overall contribution of 1.8 ± 0.1% at 18 mM SDS. The emission λ_{max} values of 433 and 521 nm correspond to the maximal wavelengths recorded for aqueous solutions of Prodan.

Prodan Distribution within SDS Micelles. Variation in Order of Reagent Addition. Addition of SDS to aqueous solutions of Prodan (to assure the presence of probe prior to micelle formation) led to an overall increase in the intensity of Prodan fluorescence. Trilinear analyses of emission spectra acquired for varying excitation wavelength and Prodan concentration yielded a single fluorescence component at 507 ± 1 nm for samples prepared by adding probe to SDS micelles and resulted in two fluorescence components at 496 ± 1 and 507 ± 1 nm for samples prepared by adding SDS to aqueous Prodan solutions. The shorter wavelength component comprised 24.3 ± 0.7% of the overall fluorescence independent of [Prodan].

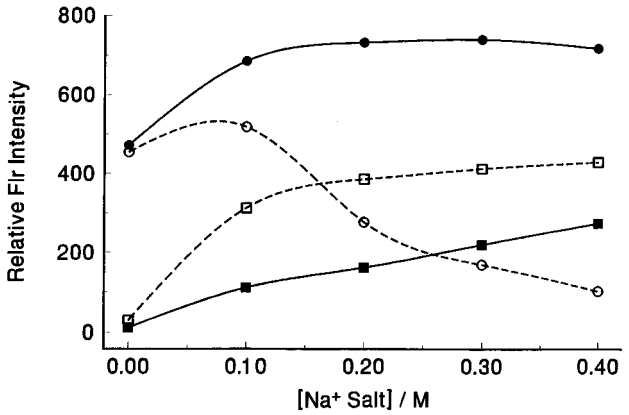

Figure 3. Dependence of the fluorescence intensity emitted by Prodan in aqueous SDS solutions on added Na^+ counterion and on the presence of the collisional quencher I^-. Prodan fluorescence is resolved by trilinear analysis into two contributing components with emission λ_{max} equal to 503 (●) and 497 nm (■) in the presence of NaCl and at 503.1 nm (○) and 501.9 nm (□) in the presence of NaI.

TABLE 2: Distinct Prodan Fluorescence Components Resolved in Cation-Treated SDS Micelles

	component 1		component 2	
counterion[a]	λ/nm[b]	%[c]	λ/nm	%
untreated	*d*		507	98
Li^+	501	16	504	84
Na^+	497	28	503	72
K^+	497	39	508	61
NH_4^+	502	79	512	21
$N(CH_3)_4^+$	496	46	502	54
$N(Ethyl)_4^+$	496	45	503	55
$N(Butyl)_4^+$	486	67	503	33

[a] Fluorescence values reported for fixed counterion concentrations: $[Li^+] = [Na^+] = [NH_4^+] = [N(CH_3)_4^+] = [N(CH_3CH_2)_4^+] = 0.40$ M; $[K^+] = 0.010$ M; and $[N(CH_3CH_2CH_2CH_2)_4^+] = 0.075$ M. [SDS] = 10 mM. [b] Emission λ_{max} values expressed with uncertainties of ±1 nm. [c] Percent values represent the percentages contributed by each component to the overall fluorescence intensity at the given [counterion]. Uncertainties in percent values are estimated to be ±1%. [d] The remaining contribution to the overall Prodan emission spectrum arises from a small amount of "free" Prodan not associated with SDS micelles.

Prodan Emission as a Function of Added [Counterion] in SDS Micelles. Increasing concentrations of added counterion (Li^+, Na^+, K^+, NH_4^+, $N(CH_3)_4^+$, $N(CH_3CH_2)_4^+$, $N(CH_3CH_2CH_2CH_2)_4^+$ added as chloride salts) increase the overall fluorescence of Prodan in micellar systems. For example, for those cations that could be added at concentration levels of 0.40 M, the fluorescence intensity at the emission λ_{max} induced by 360-nm excitation increased by a factor of 2.02 for Li^+, 2.06 for Na^+, 2.18 for NH_4^+, 3.18 for $N(CH_3)_4^+$, and 3.34 for $N(CH_3CH_2)_4^+$. Trilinear analyses of the Prodan emission in alkali metal-treated micelles and in SDS micelles treated with the ammonium tetraalkylammonium cations yielded two fluorescence components. The dependences of the components on $[Na^+]$ are illustrated in Figure 3. Table 2 summarizes the emission λ_{max} values observed and the percentage contribution of each component to the overall fluorescence. For the alkali metal series, the λ_{max} of the two components shift to shorter wavelength as the cation size increases. Furthermore, the relative fluorescence intensity of the shorter wavelength component increases in the order $Li^+ < Na^+ < K^+$. For the series of alkyl-substituted ammonium cations with increasing alkyl chain length, the results reflect an increasing contribution of shorter wavelength components to the overall fluorescence spectrum. For example, NH_4^+-treated SDS micelles exhibit two

Prodan emissions at 502 and 512 nm, while $N(CH_3CH_2CH_2CH_2)_4^+$-treated micelles display two Prodan populations with λ_{max} at 486 and 503 nm. The 502-nm component contributes 79% of the fluorescence observed in micelles with added NH_4^+ counterion, but the 503-nm Prodan emission in micelles with added tetrabutylammonium ion yields only 33% of the total fluorescence signal.

Selective Quenching of Prodan Emission in SDS Micelles. Addition of increasing concentrations of NaI led to a decrease in the overall fluorescence intensity of Prodan-treated SDS micelles. Trilinear analysis identified two Prodan fluorescence signals with similar emission λ_{max} but distinct dependences on $[I^-]$. The component emitting at slightly longer wavelength, $\lambda_{max} = 503.1$ nm (with excitation $\lambda_{max} \geq 360$ nm), was the dominant component in the absence of iodide, exhibited an increase in fluorescence intensity as $[I^-]$ increased to 0.1 M, and then decreased significantly in intensity at higher iodide concentrations. The second component, emitting maximally at 501.9 nm (with excitation $\lambda_{max} = 354 \pm 1$ nm), rose in intensity as $[I^-]$ increased and remained the dominant component for $[I^-] > \approx 0.2$ M. Figure 3 illustrates these trends. To separate the effects of the cation Na^+ from the collisional quencher I^-, Figure 3 also presents the dependence on $[Na^+]$ of the two emission components resolved for NaCl-treated SDS micelles. As $[Na^+]$ increases, the intensity of each component rises, with the longer wavelength emission (503 nm) saturating at about 0.2 M Na^+ and the shorter wavelength emission (497 nm) steadily increasing with added Na^+.

To determine the fraction of Prodan fluorescence accessible to quenching by added iodide, conventional and modified Stern−Volmer analyses[16,17] were performed. To focus solely on the effect of added I^- and not on the influence of Na^+ on the Prodan fluorescence, fluorescence intensities of NaI-treated micelles were compared with those treated with an identical concentration of NaCl. The conventional Stern−Volmer equation,

$$F_o/F = 1 + K_{SV}[I^-]$$

relates the Prodan fluorescence intensity in the absence and presence of I^-, F_o, and F, respectively. For each quencher concentration, fluorescence emission intensities at the observed λ_{max} using $\lambda_{exc} = 330$ nm were used. The data did not yield a linear fit with a y-intercept of 1, indicating incomplete accessibility of the Prodan fluorescence to quencher. The modified Stern−Volmer equation,

$$F_o/\Delta F = 1/f_a = 1/\{f_a K_{SV}[I^-]\}$$

permits the calculation of the f_a parameter, the fraction of Prodan fluorescence accessible to quenching by I^-. The value of ΔF is defined as the decrease in the Prodan fluorescence intensity induced by the given iodide concentration, i.e., $F_o - F$. The modified Stern−Volmer plot, presented in Figure 4, indicates a value of $f_a = 0.62 \pm 0.03$ and a Stern−Volmer quenching constant of 5.2 ± 0.1 M^{-1}.

Dependence of Anion of Na^+ Salt on Prodan Emission in SDS Micelles. To ascertain the dependence on Prodan emission in SDS micelles of Na^+ salts with varying anions, micellar samples with [SDS] fixed at 18 mM were treated with added sodium chloride, sodium acetate, or sodium sulfate. The fluorescence intensity at the emission λ_{max} induced by 360-nm excitation increased by a factor of 2.06 for Cl^-, 2.15 for SO_4^{2-}, and 1.97 for CH_3COO^-. SDS micelles treated with Na_2SO_4 yielded the same emission spectra as those samples with no added sodium counterion. As previously seen for NaCl, addition of sodium acetate to SDS micelles enhanced the contribution of a shorter wavelength component to the emission spectrum of Prodan, resolved via trilinear analysis. A similar effect was observed upon the addition of benzyl alcohol to SDS micelles. Trilinear analysis of Prodan emission in benzyl alcohol-treated SDS micelles revealed a two-component fit with Prodan emission at 469 and 511 nm. Table 3 summarizes the Prodan emission characteristics in these systems.

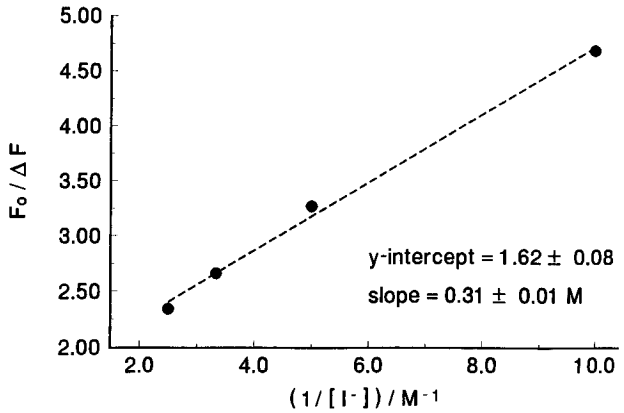

Figure 4. Modified Stern−Volmer plot to assess the fraction (f_a) of Prodan fluorescence in Na^+-treated SDS micelles that is accessible to quenching by the collisional quencher I^-. The modified Stern−Volmer equation is given by $F_o/\Delta F = 1/f_a + 1/\{f_a K_{SV}[I^-]\}$ where F_o is the Prodan fluorescence intensity in the absence of I^- and the value of ΔF is defined as the decrease in the Prodan fluorescence intensity induced by the given iodide concentration, i.e., $F_o - F$. For each quencher concentration, fluorescence emission intensities at the observed λ_{max} using $\lambda_{exc} = 330$ nm were used. The analysis yields a value of $f_a = 0.62 \pm 0.03$ and a Stern−Volmer quenching constant K_{SV} of 5.2 ± 0.1 M.

TABLE 3: Distinct Prodan Fluorescence Components Resolved in Na^+-Treated SDS Micelles[a]

	component 1		component 2	
Na^+ salt	λ/nm[b]	%[c]	λ/nm	%
none	507	97	*d*	
NaCl	504	93	483	7
Na_2SO_4	503	100		
$NaOOCCH_3$	506	88	482	12
$C_6H_5CH_2OH$[d]	511	90.6	469	9.4

[a] Fluorescence values reported for fixed counterion concentrations, $[Na^+] = 0.40$ M. [SDS] = 18 mM. [b] Emission λ_{max} values expressed with uncertainties of ±1 nm. [c] Percent values represent the percentages contributed by each component to the overall fluorescence intensity at the given [counterion]. Uncertainties in percent values are estimated to be ±1%. [d] Experiment conducted for comparison with $[C_6H_5CH_2OH] = 0.30$ M^{-1}.

Prodan Emission as a Function of [DTAB]. Fluorescence studies varying the DTAB concentration display a sizable increase in Prodan fluorescence at 1.98 mM DTAB. Trilinear analyses of the emission spectra yielded a three-component fit with Prodan emission at 436 ± 1, 497 ± 1, and 520 ± 1 nm. The emission peak at 520 nm dominates at [DTAB] below the cmc (contributing 90.0 ± 1.0% of the total fluorescence intensity at 0.50 mM DTAB), while the intensity of the 497-nm component rises dramatically above the cmc to contribute essentially 100% of the observed fluorescence at 3.00 mM DTAB. The contribution of the 435-nm emission is negligible at all [DTAB], falling from 10.0 ± 1.0 to 0.0% as [DTAB] rises from 0.50 to 3.0 mM. As observed earlier, the λ_{max} values of 436 and 520 nm correspond to the maximal wavelengths recorded for aqueous solutions of Prodan and have been attributed to emission from hydrogen-bonded and non-hydrogen-bonded Prodan molecules, respectively.

TABLE 4: SDS and DTAB Single and Mixed Micelle Systems. Emission λ_{max} Values[a] and Intensities[b] of Micelle-Associated Prodan Fluorescence Components

system	λ/nm	%	λ/nm	%	λ/nm	%	λ/nm	%	SDS/DTAB[c]
pure SDS micelles							507	100	∞
SDS-rich micelles					487	14	506	86	7.75
						16		84	3.50
						54		46	2.94
						58		42	1.50
SDS vesicles + 1:1 ppt[d]	453	15			487	85			1.33
		14				87			1.09
DTAB-rich micelles + 1:1 ppt[d]			474	13			496	87	0.667
				13				87	0.400
				11				89	0.286
DTAB-rich micelles					486	25	496	75	0.127
						21		79	0.083
						19		81	0.044
pure DTAB micelles							497	100	0.000

[a] Emission λ_{max} values expressed with uncertainties of ±1 nm. [b] Percent values represent the percentages contributed by each component to the overall fluorescence intensity at the given SDS/DTAB weight ratio. Uncertainties in percent values are estimated to be ±1%. [c] Weight ratio of SDS/DTAB. Uncertainties estimated to be ±0.01 for ratios of ≥1.00 and ±0.002 for ratios of <1.00. [d] Fluorescence measured for solution obtained after centrifugation to separate 1:1 SDS−DTAB precipitate.

Prodan Emission in Systems of SDS and DTAB. In each of the four regions of the binary SDS−DTAB phase diagram that were examined, trilinear analysis of the Prodan fluorescence emission yielded three fluorescence components corresponding to Prodan in three unique microenvironments. The λ_{max} values and percentages of the total fluorescence contributed by each component for each region are presented in Table 4. In the one-phase region of SDS-rich micelles, the contribution of the 507-nm component to the overall fluorescence spectrum decreased with increasing [DTAB], as two shorter wavelength components appeared. As the SDS/DTAB weight ratio was lowered from 7.75 to 2.94, a 492-nm component and a 471-nm component exhibited increases of 6−38 and 11−20%, respectively, in the contributions to the total fluorescence signal. In the one-phase region of DTAB-rich micelles, the contributions of the three resolved fluorescence components were independent of SDS/DTAB weight ratio: $\lambda_{max} = 498$ nm with 68 ± 1% of the total fluorescence, $\lambda_{max} = 493$ nm with 26.5 ± 0.5%, and $\lambda_{max} = 459$ nm with 5.5 ± 0.5%. The supernatant of samples in the two-phase region of DTAB-rich micelles and DTAB−SDS precipitate yielded two of the same components: $\lambda_{max} = 499$ nm with 67 ± 1% of the total fluorescence and $\lambda_{max} = 493$ nm with 22.5 ± 0.5%. The third component increased slightly in wavelength and percent contribution: $\lambda_{max} = 474$ nm with 10.5 ± 0.5%. Finally, the liquid supernatant of the two-phase region of SDS-rich vesicles and DTAB−SDS precipitate exhibited three fluorescence components with concentration-independent contributions to the overall fluorescence yield: $\lambda_{max} = 489$ nm with 67.5 ± 1.5%, $\lambda_{max} = 484$ nm with 18 ± 1%, and 453 nm with 14.5 ± 0.5%.

Discussion

Single-Surfactant Micelles. The results of this study demonstrate that the fluorescence probe Prodan is a powerful indicator of structural features of SDS and DTAB micellar systems. At low concentrations, Prodan exhibits a strong affinity for a micellar region in either SDS ($\lambda_{max} = 507$ nm) or DTAB ($\lambda_{max} = 497$ nm) aggregates, with little free Prodan in the surrounding aqueous exterior ($\lambda_{max} = 520$ nm). For both types of micelles, then, Prodan most likely resides at the water−surfactant interface, i.e., on the surface of the micelle in a polar disposition.[18] The naphthalene ring does not penetrate deep into either micelle, as a greater emission wavelength shift from an aqueous λ_{max} of 520 nm would have been expected. Our studies show that Prodan emission in ethanol, for example, occurs at 488 nm and at considerably shorter wavelength in more nonpolar solvents.

The sensitivity of Prodan fluorescence to its microenvironment is responsive enough to distinguish between the interfacial regions of SDS and DTAB micelles. The 10-nm difference in Prodan emission wavelengths for SDS and DTAB micelles is significant and most likely reflects the relative extent of water accessibility of the Prodan environments. Prodan at the interface of SDS micelles exhibits emission at a longer wavelength, consistent with a more polar microenvironment. The enhanced polarity of the surroundings can be attributed to greater water penetration of the micelle interface. In support of this interpretation, there is general agreement that micelles with anionic sulfate carboxylate head groups (e.g., SDS) are usually found to be more hydrated than those with trimethylammonium head groups (e.g., DTAB).[19]

The variable accessibility of water to Prodan at micellar interfaces can be further supported by an estimate of the surface areas per surfactant head group. The *effective* surface area per head group can be calculated by dividing the total surface area of the micelle interior by the aggregation number. For spherical micelles, the length of the hydrocarbon tail of a surfactant dictates the radius of the spherical core with the maximum radius equal to the fully extended length of the hydrocarbon tail.[20] Thus the surface area of the interior core of dodecyl groups may be considered constant for SDS and DTAB. The generally larger aggregation number for SDS micelles suggests a smaller *effective* surface area per head group for this surfactant by a factor ranging from as low as 1.04 [9] or 1.16 [12] to a high of 1.6.[5] However, our estimates of cross-sectional diameters of the tetramethylammonium cationic and sulfonate anionic head groups using Hyperchem molecular modeling software predict a ratio of *actual* surface areas for DTAB−SDS head groups of 2.37 [ratio = $(r_{DTAB}/r_{SDS})^2 = (2.0\ \text{Å}/1.3\ \text{Å})^2$]. Thus, the amount of *void* space around the DTAB head group is less than around the SDS head group, consistent with a smaller degree of water permeability for DTAB micelles. The more nonpolar environment for Prodan near the DTAB head groups is consistent with this argument.

Variations in SDS Head-Group Spacing. The distribution of Prodan within the micelle may be altered by changes in the head-group spacing on the micelle interface. For example, SDS head groups are brought closer in proximity by a reduction in the electrostatic repulsions by added counterion. Our results

suggest that an incorporation of Prodan in a slightly more nonpolar environment accompanies the modification in head-group repulsive forces with either alkali metal cations or alkyl-substituted ammonium cations. This conclusion is consistent with the observation of an increased contribution of the shorter wavelength emission component(s) to the overall Prodan fluorescence spectrum as counterion is added (Table 2). The slightly more nonpolar environment could be achieved by reduced water penetration at the micellar surface. Stern−Volmer analysis of the quenching of Prodan fluorescence in Na^+-treated SDS micelles by added iodide further suggests that the shorter wavelength fluorescence component is consistent with Prodan in an environment made more nonpolar as a consequence of reduced water penetration. Prodan held more deeply in the micellar interface with reduced contact with water could not undergo collision with iodide ions in the external aqueous solvent. As a consequence the shorter wavelength fluorescence would be inaccessible to collisional quenching by I^-.

For the alkali metal series $Li^+ \rightarrow Na^+ \rightarrow K^+$ and the tetrasubstituted ammonium ion series $NH_4^+ \rightarrow N(CH_3)_4^+ \rightarrow N(CH_2CH_3)_4^+ \rightarrow N(CH_2CH_2CH_2CH_3)_4^+$, the increasing contribution of the shorter wavelength components and the decrease in the wavelengths of the components resolved reflect decreasing exposure of Prodan to water. Water penetration at the micellar interface is more restricted with larger (e.g., K^+ vs Li^+) or more bulky (e.g., $N(butyl)_4^+$ vs NH_4^+) counterions. In particular, hydrophobic forces enhance the binding strength of the alkyl-substituted ammonium ions.[21] This interpretation is in agreement with observations in an infrared absorption study of SDS micelles that suggest a decrease in the roughness of micelle surfaces and in the extent of hydrocarbon−water contacts for the series $Li^+ \rightarrow Na^+ \rightarrow N(CH_3)_4^+ \rightarrow N(CH_2CH_3)_4^+$.[21] A small-angle neutron scattering study[22] also suggests that the $N(CH_3)_4^+$ counterion leads to less penetrating water than the Na^+ in dodecyl sulfate micelles. At variance with these findings are the results of electron spin resonance[23] and electron spin-echo modulation[24] techniques that suggest more water penetration in dodecyl sulfate micelles synthesized with an ammonium counterion (as opposed to treated with added cation) rather than a sodium counterion.

Alternatively, the SDS head groups may be pushed further apart by the interaction of bulky additives on the micelle surface such as the adsorbed benzyl alcohol or the presence of multivalent anions such as divalent SO_4^{2-}.[1,25] Benzyl alcohol markedly reduces the proportion of bound water hydrating the Na^+ counterions,[1,26] leading to greater freedom of motion for the surfactant head group and consequently to a more open micellar structure. Our results with benzyl alcohol suggest a greater incorporation of Prodan within the micelles (the percentage of fluorescence from interfacial Prodan declines from 97 to 91%) and a positioning of Prodan within a less water-accessible region (shift of λ_{max} from 507 to 469 nm). Addition of some electrolytes, such as the inclusion of Na_2SO_4 in SDS micelle samples, results in competing effects. The Na^+ counterion would be expected to diminish the electrostatic repulsion of the head groups of SDS; however, the divalent SO_4^{2-} anion apparently prevents such an effect, resulting in a Prodan emission spectrum identical to that obtained in untreated SDS micelles. The monovalent chloride and acetate ions apparently do not hinder the action of Na^+ as extensively as SO_4^{2-}, generating a pool of Prodan molecules in a more nonpolar region of the SDS micelle. On the other hand, the effect of added I^- (collisional quenching studies) on the wavelength of the more nonpolar Prodan emission component (shift from 497 to 501.9 nm as $[I^-]$ increases) is most likely another example of opposite effects of Na^+ and I^- on the head-group spacing within the SDS micelle.

Mixed Micellar Systems. The various phase regions in dilute aqueous SDS−DTAB mixtures can be distinguished by the individual components of Prodan emission resolved via trilinear analyses. As previously noted, Prodan located in pure SDS micelles emits principally at 507 nm, 10 nm above the emission of Prodan in pure DTAB micelles at 497 nm. For the isotropic one-phase regions of the binary SDS−DTAB system, solutions of SDS-rich micelles are characterized by two Prodan emissions—507 (primarily containing SDS) and 487 nm (containing significant amounts of DTAB). As DTAB is added to SDS micelles, the incorporation of DTAB within the micelle is signaled by the appearance of shorter wavelength components. The reduction in head-group spacing from the opposite charges of SDS and DTAB and the substantial growth in micellar size provide a larger and less water-accessible (i.e., more nonpolar) environment in which Prodan may reside. The increase in the contribution of the 487-nm component to the overall fluorescence most likely reflects the increase in the number of mixed micelles compared to pure SDS micelles. The lack of variation in λ_{max} with micellar size (recall aggregation number increases as DTAB is added[9]) suggests that Prodan is not necessarily partitioning deeper within the micelle as the number of surfactant molecules increases. Furthermore, since there is at most one Prodan molecule per 30 mixed micelles of the largest possible aggregation numbers (i.e., $N \approx 200$), the existence of two distinct Prodan emission wavelengths suggests two populations of Prodan molecules *not* contained within the same molecule. Therefore, the results are consistent with a heterogeneous system of pure SDS and mixed SDS−DTAB micelles at each SDS/DTAB ratio. Similarly, solutions of DTAB-rich micelles exhibit Prodan emission at 497 (chiefly DTAB-containing micelles) and 486 nm (mixed micelles of SDS and DTAB). The results are also consistent with a heterogeneous population of pure DTAB and mixed SDS−DTAB micelles. A limited growth of micelle size with varying SDS/DTAB ratio is indicated by the small increase in the contribution of the 486-nm component to the total fluorescence signal. The data provide no evidence for a deeper partitioning of Prodan within the mixed micelles as SDS is continually added, particularly due to the lack of variation in λ_{max} for Prodan in the mixed micelle.

The solution of the two-phase regions containing 1:1 DTAB−SDS precipitate and SDS vesicles is delineated by the same 487-nm emission as SDS-rich micelles and by a new shorter wavelength emission at 453 nm. As both large unilamellar and multilamellar vesicles form in SDS−DTAB mixtures[9], the 453-nm emission is consistent with Prodan in a more nonpolar environment as in the interior of a multilamellar vesicle. For the solution of the two-phase region of DTAB-rich micelles and 1:1 precipitate, the Prodan emission at 474 nm in addition to the previously observed value at 496 nm suggests a more nonpolar and/or less water-accessible region for Prodan within the micelles. Thus, each one- and two-phase region of the dilute aqueous binary SDS−DTAB pseudoternary diagram can be identified by distinct combinations of Prodan emission wavelengths.

Conclusion

These investigations are a definitive demonstration of the sensitivity and effectiveness of the fluorophore Prodan as a probe of micelle structure, including both single-surfactant and mixed micelle systems. Coupled with factor analysis techniques to resolve multiple Prodan microenvironments, the environmentally

sensitive emission characteristics of Prodan detect such characteristics as the relative polarities of the surfaces of micellar cores, the permeability of the micelle interface, and the heterogeneity of SDS−DTAB mixed micellar systems. The simultaneous partitioning of the probe Prodan into the principal regions of aqueous micelles is a promising approach to the characterization of micellar systems.

Acknowledgment. This research was supported in part by a grant from the National Science Foundation Research Experiences for Undergraduates Program (CHE-9322804). Acknowledgment is also made to the donors of the Petroleum Research Fund, administered by the American Chemical Society, for the partial support of this research. K.K.K. acknowledges the Henry Dreyfus Teacher-Scholar Awards Program for support of this research.

References and Notes

(1) Gratzel, M.; Thomas, J. K. In *Modern Fluorescence Spectroscopy 2*; Wehry, E. L., Ed.; Plenum Press: New York, 1976; Chapter 4.

(2) Weber, G.; Farris, F. J. *Biochemistry* **1979**, *18*, 3075.

(3) Torgerson, P. M.; Drickamer, H. G.; Weber, G. *Biochemistry* **1979**, *18*, 3079.

(4) Israelachvili, J. N. In *Physics of Amphiphiles: Micelles, Vesicles and Microemulsions*; Elsevier Science: New York, 1985; pp 24−58.

(5) Phillips, J. N. *Trans. Faraday Soc.* **1955**, *51*, 561.

(6) Elworthy, P. H.; Mysels, K. J. *J. Colloid Sci.* **1966**, *21*, 331.

(7) Krathovil, J. P. *J. Colloid Interface Sci.* **1980**, *75*, 271.

(8) Ottewill, R. H. In *Surfactants*; Tadros, Th. F., Ed.; Academic Press: Orlando, FL, 1984; Chapter 1.

(9) Herrington, K. L.; Kaler, E. W.; Miller, D. D.; Zasadzinski, J. A.; Chiruvolu, S. *J. Phys. Chem.* **1993**, *97*, 13792.

(10) Evans, D. F.; Wennerstrom, H. *The Colloidal Domain*; VCH Publishers: New York, 1994; Chapter 4.

(11) Jones, M. N.; Piercy, J. *J. Chem. Soc., Faraday Trans. 1* **1972**, *68*, 1839.

(12) Lianos, P.; Zana, R. *J. Colloid Interface Sci.* **1981**, *84*, 100.

(13) Leurgans, S.; Ross, R. T. *Stat. Sci.* **1992**, *7*, 289.

(14) Balter, A.; Nowak, W.; Pawelkiewicz, W.; Kowalczyk, A. *Chem. Phys. Lett.* **1988**, *143*, 565.

(15) Nowak, W.; Adamczak, P.; Balter, A.; Sygula, A. *J. Mol. Struct.* **1986**, *139*, 13.

(16) Lehrer, S. S. *Biochemistry* **1971**, *10*, 3254.

(17) Lakowicz, J. R. *Principles of Fluorescence Spectroscopy*; Plenum Press: New York, 1984; Chapter 9.

(18) Chong, P. L.-G. *Biochemistry* **1988**, *27*, 399.

(19) Hayter, J. B. In *Physics of Amphiphiles: Micelles, Vesicles and Microemulsions*; Degiorgio, V., Ed.; Elsevier Science: New York, 1985; pp 59−93.

(20) Hiemenz, P. C. *Principles of Colloid and Surface Chemistry*; Marcel Dekker: New York, 1986; Chapter 8.

(21) Abuin, E. B.; Lissi, E.; Casai, H. L. *J. Photochem. Photobiol. A: Chem.* **1991**, *57*, 343.

(22) Berr, S. S.; Coleman, M. J.; Jones, R. R. M.; Johnson, J. S., Jr. *J. Phys. Chem.* **1986**, *90*, 6492.

(23) Szajdzinska-Pietek, E.; Maldonado, R.; Kevan, L.; Jones, R. R. M. *J. Am. Chem. Soc.* **1984**, *106*, 4675.

(24) Szajdzinska-Pietek, E.; Maldonado, R.; Kevan, L.; Jones, R. R. M.; Coleman, M. J. *J. Am. Chem. Soc.* **1985**, *107*, 784.

(25) Gratzel, M.; Thomas, J. K. *J. Am. Chem. Soc.* **1973**, *95*, 6885.

(26) Roberts, R. T.; Chachaty, C. *Chem. Phys. Lett.* **1973**, *22*, 348.

JP960993G